THE JOURNAL OF BIOLOGICAL CHEMISTRY
Vol. 274, No. 30, Issue of July 23, pp. 21297–21304, 1999
Printed in U.S.A.

The Cap-binding Protein eIF4E Promotes Folding of a Functional Domain of Yeast Translation Initiation Factor eIF4G1*

(Received for publication, April 5, 1999, and in revised form, May 12, 1999)

Panda E. C. Hershey, Sarah M. McWhirter, John D. Gross‡, Gerhard Wagner‡, Tom Alber, and Alan B. Sachs§

From the Department of Molecular and Cell Biology, University of California at Berkeley, Berkeley, California 94720 and the ‡Department of Biological Chemistry and Molecular Pharmacology, Harvard Medical School, Boston, Massachusetts 02115

The association of eucaryotic translation initiation factor eIF4G with the cap-binding protein eIF4E establishes a critical link between the mRNA and the ribosome during translation initiation. This association requires a conserved seven amino acid peptide within eIF4G that binds to eIF4E. Here we report that a 98-amino acid fragment of *S. cerevisiae* eIF4G1 that contains this eIF4E binding peptide undergoes an unfolded to folded transition upon binding to eIF4E. The folding of the eIF4G1 domain was evidenced by the eIF4E-dependent changes in its protease sensitivity and ^{1}H-^{15}N HSQC NMR spectrum. Analysis of a series of charge-to-alanine mutations throughout the essential 55.4-kDa core of yeast eIF4G1 also revealed substitutions within this 98-amino acid region that led to reduced eIF4E binding *in vivo* and *in vitro*. These data suggest that the association of yeast eIF4E with eIF4G1 leads to the formation of a structured domain within eIF4G1 that could serve as a specific site for interactions with other components of the translational apparatus. They also suggest that the stability of the native eIF4E-eIF4G complex is determined by amino acid residues outside of the conserved seven-residue consensus sequence.

The recruitment of the small ribosomal subunit to the 5′-end of an mRNA molecule is often the rate-limiting step in the eucaryotic translation initiation pathway (reviewed in Ref. 1). The 5′-ends of eucaryotic mRNAs are distinguishable from other RNAs in the cell due to the presence of the $m^{7}GpppX$ (where *X* is any nucleotide) cap structure (2). This cap structure is specifically recognized by the cytoplasmic cap-binding protein eIF4E (reviewed in Ref. 3). Recruitment of the small ribosomal subunit to mRNA is facilitated by eIF4G, which interacts with eIF4E, the RNA-stimulated ATPase eIF4A, and, at least in mammalian cells, the 40 S ribosomal subunit-associated eIF3 complex (4, 5).

The association of eIF4E with eIF4G is subject to regulation (reviewed in Ref. 3). For instance, in human cells at least three different eIF4E-binding proteins (4E-BPs)[1] competitively block the association of eIF4G with eIF4E. Binding of the 4E-BPs to eIF4E in mammalian cells is regulated through a PI3-kinase-dependent and rapamycin-sensitive pathway. Phosphorylation of the 4E-BPs under growth-promoting conditions leads to their release from eIF4E, the subsequent association of eIF4G with eIF4E, and increases in cap-dependent translation. Conversely, in mammalian cells, dephosphorylation of eIF4E under conditions of cellular stress, such as heat shock or viral infection, leads to a decrease in its binding to eIF4G and capped mRNAs (6). Regulation of the phosphorylation state of eIF4E is currently thought to occur via the control of the eIF4G-associated kinase Mnk1p (7).

The yeast *Saccharomyces cerevisiae* contains a single eIF4E gene, *CDC33* (8) and two eIF4G genes, *TIF4631* and *TIF4632* (9), encoding the eIF4G1 and eIF4G2 proteins, respectively. Yeast eIF4E associates with these eIF4Gs and is responsible for mediating cap-dependent translation (10–12). *S. cerevisiae* also contains at least one 4E-BP, encoded by the *CAF20* gene, which functions as a negative regulator of the eIF4E-eIF4G interaction (13, 14). Although both eIF4E and Caf20p are phosphoproteins, the physiological relevance of their modifications remains unknown (15).

Pioneering studies on the regions of eIF4G and the 4E-BPs that interact with eIF4E identified a consensus binding sequence, Y*XXXX*LΦ (where *X* is any amino acid and Φ is an aliphatic residue), common to eIF4G and the 4E-BPs (16). This conserved sequence (which will be referred to here as the eIF4E binding peptide) is necessary for eIF4E binding (for instance, see Refs. 16 and 17). The x-ray crystal structure of a ternary complex between the cap, eIF4E, and a 17-residue peptide containing the eIF4E binding peptide of 4E-BP1 revealed that the eIF4E binding peptide associates directly with a conserved surface of eIF4E.[2] Based on the findings that mutations in eIF4E have differential effects on the binding of eIF4G and Caf20p, it has been suggested that the interactions of eIF4G and the 4E-BPs with eIF4E are not limited to the eIF4E binding peptide (19).

The association of eIF4G with eIF4E has been shown to significantly enhance the affinity of eIF4E for the cap structure (20). As the level of functional eIF4E (*i.e.* not bound to 4E-BP) is considered to be one of the limiting factors during the translation initiation process, this discovery suggested that the eIF4E-eIF4G interaction serves not only to bridge the ribosomal subunit to the mRNA but also to increase the effective

* This work was supported in part by NIH Grant 50308 (to A. B. S.). The costs of publication of this article were defrayed in part by the payment of page charges. This article must therefore be hereby marked "*advertisement*" in accordance with 18 U.S.C. Section 1734 solely to indicate this fact.

§ To whom correspondence should be addressed: Dept. of Molecular and Cell Biology, 401 Barker Hall, University of California at Berkeley, Berkeley, CA 94720. Tel.: 510-643-7698; Fax: 510-643-5035; E-mail: asachs@uclink4.berkeley.edu.

[1] The abbreviations used are: 4E-BP, eIF4E-binding protein; PAGE, polyacrylamide gel electrophoresis; PMSF, phenylmethylsulfonyl fluoride; PBS, phosphate-buffered saline; HA, hemagglutinin; LUC, luciferase; capLUC, luciferase mRNA containing a cap structure; LUCpA, luciferase mRNA containing a poly(A) tail; capLUCpA, luciferase mRNA containing both a cap structure and a poly(A) tail; GST, glutathione *S*-transferase.

[2] J. Marcotrigiano, A.-C. Gingras, N. Sonenberg, and S. K. Burley, submitted for publication.

concentration of eIF4E within the cell. The eIF4G protein is also associated with other translation initiation factors, including the poly(A) tail-binding protein Pab1p (10), the RNA-stimulated ATPase eIF4A (21, 22), and at least in mammalian cells, eIF3 (for instance, see Ref. 21). The effects of these proteins, when bound to eIF4G, on the affinity of eIF4E for the cap structure remains unknown.

In order to define the structural basis for the eIF4E-eIF4G interaction, we have undertaken a detailed analysis of the *S. cerevisiae* eIF4G-eIF4E complex. This information will help us to understand how the interaction between eIF4E and eIF4G occurs and is regulated, how this interaction leads to alterations in eIF4E affinity for the cap structure, and how other eIF4G-binding proteins could affect the eIF4G-eIF4E interaction. Here, we report that the association of eIF4E with eIF4G1 results in the formation of a protease-resistant, 98-residue fragment of eIF4G1. This fragment was shown by NMR analysis to be unfolded in the absence of eIF4E and nearly completely folded in the presence of eIF4E. Characterization of charge-to-alanine mutations within the essential 55.4-kDa region of eIF4G1 identified two mutations within this 98-amino acid fragment that resided outside of the consensus eIF4E binding peptide and that decreased eIF4G binding to eIF4E *in vivo* and *in vitro*. These data support the hypothesis that in addition to the previously defined eIF4E binding peptide, flanking regions of eIF4G1 are necessary for binding to eIF4E with high affinity. Moreover, eIF4E binding results in folding of a substantial domain of eIF4G. These results suggest a model in which eIF4E binding creates a new binding surface on eIF4G1 that may allow for the binding of other components of the translational machinery.

EXPERIMENTAL PROCEDURES

Expression and Protein Purification for Proteolysis Studies—Genes encoding the GST-eIF4G1 fusion proteins were created as follows. The eIF4G1 fragment $eIF4G1_{381–506}$ was amplified by polymerase chain reaction amplification from yeast genomic DNA with the 5′ primer CGGGATCCGAAGTTGAGGCTGAAGC and the 3′ primer CGGAATTCTCAACGACTAGAATTATTGCCG. The amplified DNA fragment was cut with *Bam*HI and *Eco*RI and ligated into a similarly digested pGEX2TK vector (Amersham Pharmacia Biotech). $eIF4G1_{393–490}$ was made using the above construct as a template for polymerase chain reaction amplification with the 5′ primer CGGGATCCATTGGACTTGAAGCTGAAATCG and the 3′ primer CGGAATTCTCATCTGCCCATTCCTGGTGG. The polymerase chain reaction amplified fragment was digested with *Bam*HI and *Eco*RI and ligated into *Bam*HI/*Eco*RI double digested pGEX2T (Amersham Pharmacia Biotech).

Strain BAS3428, which is bacterial strain BL21 containing the GST-$eIF4G1_{381–506}$, was induced at A_{600} = 0.6–0.7 with 0.5 mM isopropyl-1-thio-β-D-galactopyranoside. Cells from 1 liter of culture were resuspended in 40 ml of 50 mM Tris, pH 8.0, 20 mM NaCl, 0.5 mM EDTA, 1.0 mM PMSF, 1.0 μM leupeptin, 1.0 μM pepstatin, and 200 μg/ml lysozyme and lysed by sonication in a dry ice/ethanol bath. The suspension was centrifuged at 10,000 × *g* for 10 min at 4 °C. The pellet, which contained the majority of the induced fusion protein, was used for an inclusion body preparation. The pellet was resuspended in 80 ml of 50 mM Tris, pH 8.0, 20 mM NaCl, 0.5 mM EDTA, 0.5% Nonidet P-40, and 0.5% deoxycholic acid, briefly sonicated, and centrifuged at 10,000 × *g* for 10 min at 4 °C. The pellet was solubilized in 100 ml of 6 M guanidine hydrochloride, 200 mM Tris, pH 8.0, and then dialyzed *versus* 6 liters of phosphate-buffered saline (PBS). Following clarification by centrifugation, the supernatant was loaded onto a 10 ml Glutathione-Sepharose 4B column (Amersham Pharmacia Biotech) equilibrated in PBS. The column was washed in 5 column volumes of PBS and incubated at room temperature with 10 ml of PBS containing 10 NIH units/ml thrombin (Sigma) for 2 h. The eluted $eIF4G1_{381–506}$ was concentrated by centrifugation in a Centricon 3 device (Amicon).

Recombinant yeast eIF4E (23) was purified as described previously (24) from strain BAS2024. Briefly, cells from 1 liter of culture were resuspended in 30 ml of 20 mM HEPES, pH 7.5, 500 mM KCl, 0.2 mM EDTA, 0.5% Nonidet P-40, 1.0 mM PMSF, 1.0 μM leupeptin, 1.0 μM pepstatin, and 200 μg/ml lysozyme, lysed by sonication in a dry ice/ethanol bath, and centrifuged at 10,000 × *g* for 10 min at 4 °C. The pellet was resuspended in 60 ml of 20 mM HEPES, pH 7.5, 100 mM KCl, 0.2 mM EDTA, 0.5% Nonidet P-40, 1.0% deoxycholic acid, briefly sonicated, and centrifuged. The resulting pellet was dissolved in 30 ml of 6 M guanidine hydrochloride, 200 mM Tris, pH 8.0, and dialyzed into 20 mM HEPES, pH 7.5, 100 mM KCl, and 0.2 mM EDTA (Buffer A). This was loaded onto a 15-ml m^7GDP column equilibrated in Buffer A, washed in 5 column volumes of Buffer A, washed in 2 column volumes of Buffer A + 0.1 mM GDP, and then eluted with Buffer A + 0.1 mM m^7GDP. Pooled fractions (typically 15 ml) were concentrated using a collodian concentrator (Schleicher and Shuell).

Trypsin Digestion and Analysis—Digests were performed using purified recombinant yeast eIF4E and $eIF4G1_{381–506}$. 0.5 mg/ml total substrate protein (equimolar eIF4E and $eIF4G1_{381–506}$ or $eIF4G1_{381–506}$ alone) were incubated in 10 μl with 1:50, 1:500, or 1:5000 w/w trypsin (Sigma) in 100 mM Tris, pH 8.8, for 1.5 h at 25 °C. Reactions were stopped by addition of SDS-PAGE loading buffer and immediately boiled for 5 min. Reactions were visualized on a 12% SDS-PAGE gel stained with Coomassie Brilliant Blue.

To identify the boundaries of the eIF4G1 subfragment present in the eIF4E/$eIF4G1_{381–506}$ complex digestion (1:500 w/w trypsin), both microsequencing and mass spectrometry were used. For N-terminal microsequencing, the sample was electrophoresed on a 12% SDS-PAGE gel, transferred to a 0.45 μm polyvinylidene difluoride membrane, and microsequenced using an Applied Biosystems 477A protein sequencer. The exact mass and purity of the eIF4G1 fragment were assessed by electrospray mass spectrometry. The digest was separated by reversed-phase high pressure liquid chromatography on a Vydac semipreparative C_{18} column using linear gradients of acetonitrile in water, both containing 0.1% trifluoroacetic acid. The mass of the $eIF4G_{393–490}$ measured was within 0.5 atomic mass units of expected values.

Purification of Proteins for NMR Studies—BL21 cells containing the GST-$eIF4G1_{393–490}$ fusion protein (BAS3430) were grown in M9 minimal medium with ampicillin at 37 °C to an A_{600} of 0.5, and then induced with 1 mM isopropyl-1-thio-β-D-galactopyranoside. For isotope labeling, the M9 medium was supplemented with ^{15}N labeled ammonia (1 g/L). The cell pellet from 1 liter of medium was resuspended in 25 ml of 100 mM Tris, pH 8.0, 1 mM EDTA, 1 mM dithiothreitol, 1.0 μM pepstatin, 1.0 μM leupeptin, and 1.0 mM PMSF. Cells were lysed with a French press (three times) and centrifuged at 10,000 rpm in a SS-34 rotor for 30 min. Pellets were resuspended in 50 ml of detergent buffer containing 100 mM Tris, pH 8.0, 0.5% Nonidet P-40 and 0.5% deoxycholic acid. After centrifugation at 10,000 rpm for 30 min in a SS-34 rotor, pellets were solubilized in 5 ml of 6 M guanidine HCl, 200 mM Tris, pH 8.0. The solubilized protein was then diluted at 1 ml/min into 400 ml of refolding buffer consisting of 0.8 M arginine HCl, 200 mM Tris base, and 10 mM EDTA, pH 8.0 with slow stirring at 4 °C. The fusion protein from 1 liter of starting medium (~ 35 mg) was purified on a 6-ml glutathione-Sepharose (Amersham Pharmacia Biotech) column as described above and cleaved with 7 NIH units/mg of fusion protein of hThrombin (Sigma) in 8 ml of PBS, pH 7.4. Eluted $eIF4G1_{393–490}$ in PBS with 0.5 M NaCl was loaded onto two columns in series containing 4 ml of benzamidine-Sepharose (Amersham Pharmacia Biotech) equilibrated in PBS and 0.5 M NaCl. The $eIF4G1_{393–490}$ eluate was then dialyzed against 20 mM HEPES, pH 7.5, containing 100 mM KCl.

For the eIF4E used in the NMR experiments, the entire eIF4E open reading frame from the yeast *CDC33* gene was subcloned into the pGEM.2 vector (Promega), and this construct was transformed into the BL21 (DE3) *E. coli* strain (Novagen) to yield BAS3431. This strain was grown in M9 minimal medium with ampicillin at 37 °C and induced at 25 °C with 1 mM isopropyl-1-thio-β-D-galactopyranoside overnight. The expression level was typically 10 mg/liter. For preparation of the eIF4G1-eIF4E complex, the cells were lysed with a French press and centrifuged at 10,000 rpm in a SS-34 rotor for 30 min. The supernatant containing eIF4E (~10 mg) was loaded onto a 4-ml m^7GDP-agarose affinity column in a buffer containing 100 mM KCl, 0.5% Nonidet P-40, 1 mM PMSF, 1 mM EDTA, and 20 mM HEPES, pH 7.5. The column was then washed with 100 mM KCl, 20 mM HEPES, pH 7.5, at a flow rate of 3 ml/min for 40 min, followed by the addition of 20 ml of 0.1 mM GDP in 100 mM KCl, 20 mM HEPES. $eIF4G1_{393–490}$ (~ 5 mg) in 20 mM HEPES (pH 7.5) was then added at a flow rate of 1 ml/min. The complex was eluted with 0.2 mM m^7GDP in 100 mM KCl, 20 mM HEPES. The eluate was then dialyzed into PBS, pH 7.4, and further purified by gel filtration over a 120 ml (diameter = 1.6 cm) HiLoad 16/60 Superdex-75 column (Amersham Pharmacia Biotech).

NMR Spectroscopy—^1H-^{15}N-HSQC spectra for free ^{15}N-labeled $eIF4G_{393–490}$ and for the complex of ^{15}N-labeled $eIF4G_{393–490}$ and unlabeled eIF4E were recorded on a Bruker AMX 500 spectrometer at 26 °C, pH 7.5. The sample concentrations were 0.2 mM in PBS.

TABLE I
Bacterial strains

Bacterial strain (BAS)	Plasmid
542	p*TRP1CEN*
2003	p*TIF4631URA3CEN*
2004	p*TIF4632URA3CEN*
2024	p*CDC33*(18)
2027	pGST-eIF4G1
3113	p*tif4631-L459AL460ATRP1CEN*
3140	pGST-eIF4G1-L459AL460A
3157	p*(HA)TIF4631TRP1CEN*
3158	p*(HA)tif4631-L459AL460ATRP1CEN*
3268	p*(HA)tif4631-D407AD408ATRP1CEN*
3269	p*(HA)tif4631-E427AD428ATRP1CEN*
3270	p*(HA)tif4631-K446AK447ATRP1CEN*
3271	p*(HA)tif4631-D464AK465ATRP1CEN*
3272	p*(HA)tif4631-R495AD496ATRP1CEN*
3273	p*(HA)tif4631-D519AD520ATRP1CEN*
3274	p*(HA)tif4631-K529AR530ATRP1CEN*
3275	p*(HA)tif4631-K533AR534ATRP1CEN*
3276	p*(HA)tif4631-R539AR540ATRP1CEN*
3277	p*(HA)tif4631-D550AR551ATRP1CEN*
3278	p*(HA)tif4631-E560AK561ATRP1CEN*
3279	p*(HA)tif4631-E569AE570ATRP1CEN*
3280	p*(HA)tif4631-K588AK589ATRP1CEN*
3282	p*(HA)tif4631-R610AK611ATRP1CEN*
3283	p*(HA)tif4631-D660AE661ATRP1CEN*
3284	p*(HA)tif4631-K677AE678ATRP1CEN*
3286	p*(HA)tif4631-D715AK716ATRP1CEN*
3288	p*(HA)tif4631-R743AR744ATRP1CEN*
3289	p*(HA)tif4631-R771AR772ATRP1CEN*
3290	p*(HA)tif4631-K775AD776ATRP1CEN*
3291	p*(HA)tif4631-E783AE784ATRP1CEN*
3293	p*(HA)tif4631-K858AK859ATRP1CEN*
3294	p*(HA)tif4631-E872AE873ATRP1CEN*
3295	p*(HA)tif4631-R888AR889ATRP1CEN*
3412	pGST-eIF4G1-E427AD428A
3413	pGST-eIF4G1-K446AK447A
3428	pGST-eIF4G1$_{381–506}$
3429	pGST-eIF4G1$_{393–490}$
3430	pT7::*CDC33*

Construction of Charge-to-Alanine Mutants—Polymerase chain reaction mutagenesis was used to introduce the alanine codons into the recombinant eIF4G1 gene (10) by the method of Barettino *et al.* (25). A single mutagenic oligonucleotide and two other oligonucleotides that flanked the *Bam*HI and *Eco*RI sites of the eIF4G1 gene were used. The correct DNA sequence within 50 nucleotides of either side of the site of the mutations was confirmed by DNA sequencing.

Yeast Techniques—Mutant eIF4G1 genes (Table I) were introduced into the indicated yeast strains (Table II) by lithium acetate transformation and subsequent plating on YM-Trp medium (26). Transformants that had lost their wild type version of eIF4G1 (YAS2095) or eIF4G2 (YAS2229 and YAS2282) were selected for on YM-Trp medium containing 1 mg/ml 5-fluoroorotic acid (27).

In Vitro Translation Assays—Translation extracts from yeast expressing the HA epitope-tagged eIF4G1 were prepared as described previously (28). For all experiments, extracts were adjusted to 2 mM EGTA and were not treated with micrococcal nuclease. Translation assays were performed as described previously (28) with the following modifications: 200 ng of LUC mRNA was utilized, and the incubation of the 15 μl reaction mixture was carried out at 24 °C for 30 min. Production of luciferase was occurring linearly at this time. For experiments shown in Fig. 4, *B* and *C,* the extracts were incubated with cap analog (New England Biolabs) and recombinant eIF4E (17), respectively, for 15 min at 4 °C prior to mRNA addition. The data shown are representative of results from at least four experiments.

eIF4G-eIF4E Binding Studies—For the experiments described in Fig. 5*A,* the anti-HA monoclonal antibody 12CA5 was coupled to protein A-agarose (Santa Cruz Biotechnology) as described previously (10). 50 μl of a 50% suspension of this was incubated with 50 μl of yeast translation extract containing the HA epitope-tagged eIF4G1 protein and 200 μl of PBS + 0.1% Triton X-100. Bound eIF4G1 and its associated proteins were eluted from the resin with 25 μl of SDS-PAGE loading buffer and separated by SDS-PAGE on a 10% polyacrylamide gel. The eIF4G1 and eIF4E proteins were detected by Western analysis as described previously (17).

For studies involving GST-4G1 proteins, each *TIF4631* gene was inserted into the *Bam*HI/*Eco*RI sites of the pGEX2T expression vector (Amersham Pharmacia Biotech) and expressed in bacterial strain BL21 (see Table I). At A_{600} = 0.5, cultures were induced with 0.5 mM isopropyl-1-thio-β-D-galactopyranoside, harvested after 3 h, washed once in Buffer C (150 mM NaCl, 16 mM Na_2HPO_4, 4 mM NaH_2PO_4, pH 7.3) and quick-frozen in liquid N_2 in 1/100 the volume of the original culture. 0.5-ml aliquots were thawed, adjusted to 4 mM dithiothreitol and 2 mM PMSF, treated with 400 μg/ml lysozyme, and lysed gently by brief sonication. Clarified lysates were incubated with 40 μl of 50% suspension of glutathione-Sepharose 4B resin (Amersham Pharmacia Biotech) pre-equilibrated in Buffer C + 0.1% Triton X-100 (Buffer CT). The resin containing the bound eIF4G1 protein was then washed three times in 1 ml of Buffer CT before performing the experiments described below.

For the experiments described in Fig. 5*B,* the washed resin was resuspended in 200 μl of Buffer CT containing 5 μg of recombinant eIF4E (17) and incubated for 1 h at 4 °C. Following three washes in 1 ml of Buffer CT, the bound proteins were eluted 50 μl of SDS-PAGE loading buffer and separated by SDS-PAGE on a 10% polyacrylamide gel. The eIF4G and eIF4E proteins were detected by Western analysis as described previously (17).

The experiments described in Fig. 5*C* were performed in a manner similar to that previously described (17). Briefly, the eIF4G1 proteins were eluted from the washed resin with 50 μl of SDS-PAGE loading buffer, resolved by SDS-PAGE on 10% polyacrylamide gel, and electroblotted onto Hybond ECL nitrocellulose (Amersham Pharmacia Biotech). Following blocking with BLOTTO, the membrane with the immobilized eIF4G1 was probed with recombinant eIF4E (1 μg/ml) in Blotto, and the bound eIF4E was detected by Western analysis.

RESULTS

Limited Proteolysis of the eIF4G1-eIF4E Complex—Deletion analysis of the yeast eIF4G1 protein defined a region of approximately 100 residues (between residues 400 and 500) that is required for binding to eIF4E (10). This region contains the eIF4E binding peptide. A recombinant fragment containing this region will be referred to as eIF4G1$_{381–506}$. To characterize further the structure of the eIF4G1-eIF4E complex, we performed a protease trimming experiment on both eIF4G1$_{381–506}$ alone and a stoichiometric complex of eIF4G1$_{381–506}$ and eIF4E. In these experiments, equal amounts (by weight) of either eIF4G1$_{381–506}$ or the eIF4G1$_{381–506}$-eIF4E complex were incubated with different amounts of trypsin for a fixed time. Following inactivation of the protease, the reaction products were resolved by SDS-PAGE (Fig. 1*A*). At a concentration of trypsin that degraded the majority of eIF4G1$_{381–506}$ in the absence of eIF4E, there appeared a resistant smaller fragment of eIF4G1$_{381–506}$ when it was incubated with eIF4E (Fig. 1*A, filled circle,* compare *lane 2* with *lane 7*).

The sequence boundaries of the protected fragment within eIF4G1$_{381–506}$ were determined by mass spectrometry and microsequencing (Fig. 1*B*). The N terminus of the degraded product mapped to residue 393, and the C terminus mapped to residue 490. Contained within the fragment is the eIF4E binding peptide (residues 454–460). Importantly, the fragment contains multiple protected residues that could have been cleaved by trypsin and that lie outside of the eIF4E binding peptide region (Fig. 1*B, open circle*). The protection of these residues from digestion in the presence but not the absence of eIF4E indicated that they become inaccessible upon the formation of the eIF4G-eIF4E complex.

The Unfolded eIF4G1$_{393–490}$ Fragment Becomes Structured in the Presence of eIF4E—The identification of a 98-residue protease-resistant eIF4G1 fragment within the eIF4G-eIF4E complex was surprising because recent work has shown that the eIF4E binding peptide and several flanking residues interact with a considerable portion of the conserved surface of eIF4E that is not involved in binding to the cap structure.[2] Our protease protection data implied that a greater portion of eIF4G1 is directly bound to eIF4E than had been previously supposed and/or that the eIF4E binding domain of eIF4G1

TABLE II
Yeast strains

Yeast strain (YAS)[a]	Mutation[b]/plasmid (BAS)[c]
2095	*tif4631*::*LEU2 cdc33–1 pTIF4631URA3CEN* (2003)
2137	*tif4631*::*LEU2 tif4632*::*ura3* p*(HA)tif4631L459AL460ATRP1CEN* (3158)
2229	*tif4631*::*LEU2 tif4632*::*ura3 caf20*::*ura3* p*TIF4632URA3CEN* (2004)
2282	*tif4631*::*leu2hisg tif4632*::*ura3* p*TIF4632URA3CEN* (2004)
2416	YAS2095 + p*(HA)TIF4631TRP1CEN* (3157)
2417	YAS2095 + p*(HA)tif4631-E427AD428ATRP1CEN* (3269)
2418	YAS2095 + p*(HA)tif4631-K446AK447ATRP1CEN* (3270)
2419	YAS2095 + p*tif4631-L459AL460ATRP1CEN* (3113)
2420	YAS2095 + p*TRP1CEN* (542)
2421	*tif4631*::*leu2hisg tif4632*::*ura3* p*(HA)TIF4631TRP1CEN* (3157)
2422	*tif4631*::*leu2hisg tif4632*::*ura3* p*(HA)tif4631-E427AD428ATRP1CEN* (3269)
2423	*tif4631*::*leu2hisg tif4632*::*ura3* p*(HA)tif4631-K446AK447ATRP1CEN* (3270)
2424	*tif4631*::*leu2hisg tif4632*::*ura3* p*tif4631-L459AL460ATRP1CEN* (3113)
2425	*tif4631*::*LEU2 tif4632*::*ura3 caf20*::*ura3* p*(HA)TIF4631TRP1CEN* (3157)
2426	*tif4631*::*LEU2 tif4632*::*ura3 caf20*::*ura3* p*(HA)tif4631-E427AD428ATRP1CEN* (3269)
2427	*tif4631*::*LEU2 tif4632*::*ura3 caf20*::*ura3* p*(HA)tif4631-K446AK447ATRP1CEN* (3270)
2428	*tif4631*::*LEU2 tif4632*::*ura3 caf20*::*ura3* p*tif4631-L459AL460ATRP1CEN* (3113)

[a] The YAS number is to be used for requesting strains.
[b] All strains have the following genotype: MAT**a***ade2 his3 leu2 trp1 ura3 pep4*::*HIS3*.
[c] BAS refers to the bacterial strain number that contains the indicated plasmid.

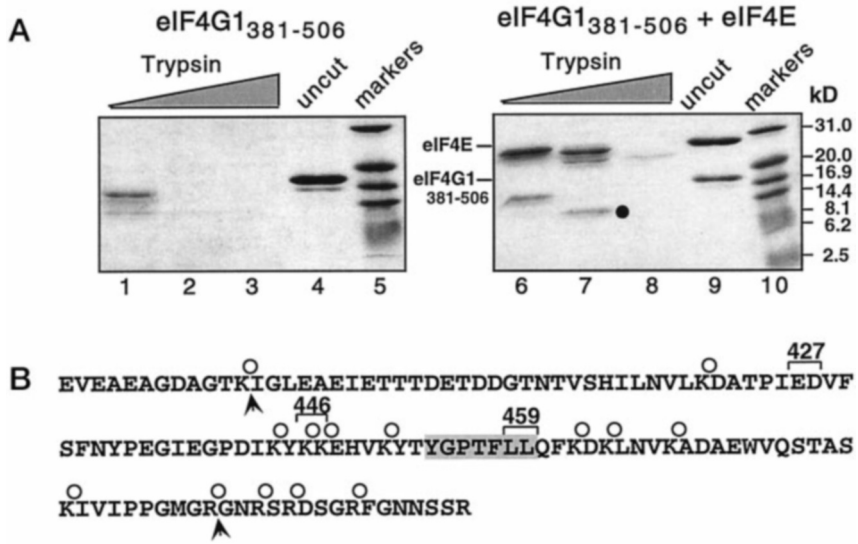

FIG. 1. **Identification of eIF4G1$_{393–490}$ as a protease-resistant fragment.** *A,* proteolysis of eIF4G1$_{381–506}$ in the presence and absence of eIF4E. Approximately 0.5 mg/ml of either eIF4G1$_{381–506}$ or eIF4G1$_{381–506}$ + eIF4E in a 1:1 stoichiometric complex was degraded with trypsin at an enzyme:substrate ratio (w/w) of 1:5000 (*lanes 1* and *6*), 1:500 (*lanes 2* and *7*), or 1:50 (*lanes 3* and *8*). Products were resolved on a 12% SDS-PAGE gel and visualized by Coomassie Brilliant Blue staining. Samples of undigested substrate (*uncut*) and molecular weight standards are also shown. The position of the stabilized eIF4G1$_{393–490}$ fragment is indicated by a *filled circle*. *B,* amino acid sequence of eIF4G1$_{381–506}$. The locations of all possible tryptic digestion sites are marked (○), as are the positions of the sites of cleavage in eIF4G1$_{393–490}$ (↑). Also marked are the locations of the eIF4G1–427, -446, and -459 mutations. The conserved eIF4E binding peptide is indicated by *shading*. Note that the amino acid numbering scheme for all eIF4G1 proteins in this report includes the two amino acids introduced at the N terminus of the recombinant protein (10).

forms a folded structure when the eIF4E binding peptide binds to eIF4E. To help distinguish among these possibilities, we wished to determine whether the eIF4G1$_{393–490}$ fragment was folded or unfolded in the absence of eIF4E and/or whether binding to eIF4E induced any changes in the structure of eIF4G1$_{393–490}$. Previous work showing that the mammalian 4E-BP1 was unfolded in the absence of eIF4E, and remained so in the presence of eIF4E provided the impetus for this investigation (29).

NMR experiments capable of determining whether the amide protons in the eIF4G1$_{393–490}$ are in a folded or unfolded conformation were performed. The isotopic labeling of the eIF4G1$_{393–490}$ fragment with ^{15}N allowed for a selective determination of the chemical environment of the amide protons of this protein in the presence or absence of unlabeled eIF4E. The amide protons of the eIF4G1$_{393–490}$ fragment exhibited few, if any, structural constraints in the absence of eIF4E (Fig. 2*A*). In contrast, when eIF4G1$_{393–490}$ was mixed with eIF4E, it yielded a ^{1}H-^{15}N HSQC NMR spectrum characteristic of a folded protein. The large number of cross-peaks appearing in the amide proton region of the spectrum of this mixture indicated that most of the 98 residues were in a structured environment. These data, in combination with the protease protection data, support the general conclusion that eIF4G1$_{393–490}$ exists as an unfolded protein in the absence of eIF4E and becomes folded in the presence of eIF4E.

Charge-to-Alanine Mutagenesis of eIF4G1 Reveals New Residues Involved in eIF4E Binding in Vivo—The physical characterization of the eIF4G1$_{393–490}$-eIF4E complex strongly suggested that residues outside of the eIF4E binding peptide could be involved in eIF4E binding. In order to examine this possibility in the full-length eIF4G1 protein and to potentially identify specific residues involved in eIF4E binding, we determined the effects on eIF4E binding of charge-to-alanine mutations

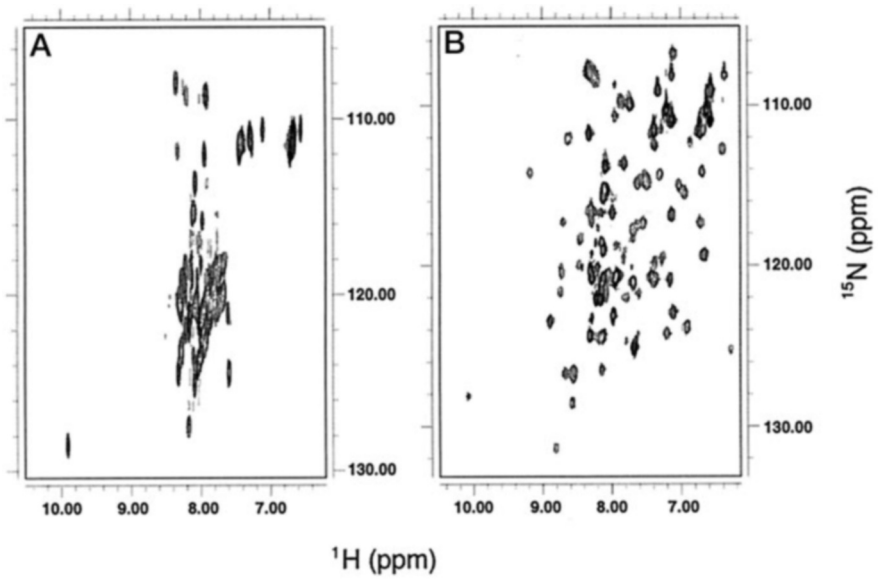

FIG. 2. **The eIF4G1$_{393–490}$ polypeptide gains structure in the presence of eIF4E.** Portions of the ^{1}H-^{15}N HSQC spectra of ^{15}N-labeled free eIF4G1$_{393–490}$ (*A*) and ^{15}N-labeled eIF4G1$_{393–490}$ complexed to unlabeled eIF4E (*B*) are shown. In the free protein, the ^{1}H-^{15}N cross-peaks are poorly dispersed, as is typical for an unfolded polypeptide. The central unresolved feature represents all the peptide amide protons, the peaks at the *upper right* are due to side chain amino protons, and the single peak at the *lower left* represents the tryptophan side chain amide proton. In the complex with eIF4E, the spectrum is dispersed, particularly in the peptide amide proton region, as is typical for a folded protein.

within eIF4G1. Twenty-four eIF4G1 mutant proteins containing two alanine residues substituted for two neighboring charge residues within the essential 55.4-kDa core of the protein (residues 400–889) (30) were analyzed (Fig. 3*A*). All but two of these mutant proteins (encoded by *tif4631-D660AE661A* and *tif4631-R743AR744A*) supported cell viability as the sole source of cellular eIF4G (data not shown).

Previous characterization of the eIF4G1–459 mutant protein (17), which contains alanine substitutions for the conserved Leu-Leu residues within the eIF4E binding peptide, prompted us to use *in vivo* and *in vitro* assays capable of detecting decreases in the functional and physical association of eIF4G1 with eIF4E. One *in vivo* test takes advantage of the observation that disruption of the eIF4G1 gene exhibits synthetic lethality when combined with the eIF4E mutation *cdc33–1*, which contains a Gly to Asp substitution at residue 113 (14). Another *in vivo* test takes advantage of the observation that loss of the yeast 4E-BP Caf20p suppresses the temperature-sensitive growth phenotype of the eIF4G1–459 mutant (17). The suppression is presumed to be due to the increased levels of free eIF4E in the cell, which through mass action increases the amount of the eIF4G1-eIF4E complex.

We discovered using a plasmid shuffling assay that combining the eIF4G1–459 mutation with the *cdc33–1* mutation led to synthetic lethality (Fig. 3*B*). This is presumably due to the negative effects of both mutations on the eIF4G1-eIF4E interaction (17). A simultaneous analysis of the ability of each of the 24 eIF4G1 mutant proteins to exhibit synthetic lethality with the *cdc33–1* mutation identified two such mutations: eIF4G1–427 and eIF4G1–446 (Fig. 3*B*). The slow growth phenotype at 37 °C of eIF4G1–427 suggested that this was the more deleterious of the two mutations. This slow growth phenotype was suppressed when the eIF4G1–427 mutant strain was deleted for the *CAF20* gene (Fig. 3*C*). These genetic data suggested that the eIF4G1–427 and -446 proteins were deficient in binding to eIF4E *in vivo*.

eIF4G1–427 and -446 Exhibit Diminished eIF4E Binding in Vitro—Several *in vitro* assays were used to determine whether the association of the mutant eIF4G1 proteins and eIF4E was deficient in crude yeast lysates (17). One of these assays takes advantage of several unique properties of translation extracts derived from the eIF4G1–459 or *cdc33–1* mutant strains. The distinguishing properties include a large stimulation of translation of uncapped mRNA translation, suppression of this effect by the addition of excess recombinant eIF4E, and the resistance of capped mRNA translation to the addition of the cap analog m^{7}GpppG.

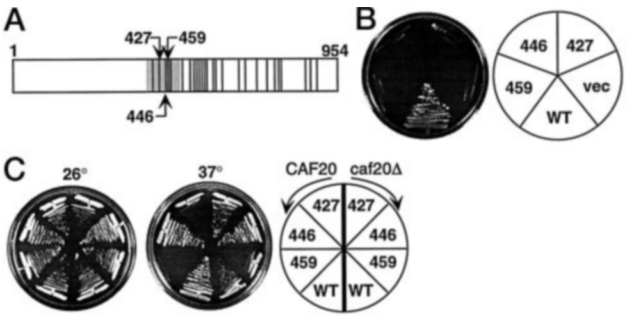

FIG. 3. **Charge-to-alanine mutagenesis of eIF4G1 reveals new residues needed for eIF4E function *in vivo*.** *A,* a diagram of the 954-amino acid yeast eIF4G1 protein used in this study is shown. The positions of each of the tandem alanine substitutions for two neighboring charged residues are represented by *vertical lines*. The location of the eIF4G1-L459AL460A mutation is also shown. The protected 98-amino acid fragment is shaded, and the locations of the eIF4G1–427, -446, and -459 mutations are noted. *B,* synthetic lethal interactions between *cdc33–1* and the eIF4G1–427, -446, and -459 mutations. Yeast strains YAS2416–2420, which contain the wild type eIF4G1 gene on a *URA3CEN* plasmid and each of the indicated eIF4G1 genes on a *TRP1CEN* plasmid, were plated on a minimal medium plate containing 5-fluoroorotic acid and incubated at 26 °C for 13 days. *WT,* wild type eIF4G1; *vec,* empty *TRP1CEN* plasmid. *C,* deletion of the yeast 4E-BP Caf20p suppresses the slow growth phenotype of the eIF4G1–427 mutation at 37 °C. Yeast strains YAS2421–2428 were plated on minimal medium plates and incubated at 26 °C (3 days) and 37 °C (5 days).

Translation extracts derived from the wild type and eIF4G1–427, -446, and -459 mutants were tested for each of these properties. In these experiments, non-nuclease-treated translation extracts were programmed with one of four mRNAs encoding the LUC protein. These mRNAs, which were generated *in vitro* using phage T3 RNA polymerase, contained a cap structure (capLUC), a poly(A) tail (LUCpA), both (capLUCpA), or neither (LUC). Following incubation of the extracts under conditions that allow for protein synthesis, the amount of LUC mRNA expression was determined with a luminescence assay (Fig. 4*A*). The eIF4G1–446 extract and the wild type extract showed similar translational properties. In contrast, the translational properties of extracts from the eIF4G1–427 and eIF4G1–459 mutants were nearly indistinguishable. Specifically, both of these mutant extracts exhibited large amounts of uncapped mRNA translation (compare LUC and LUCpA ex-

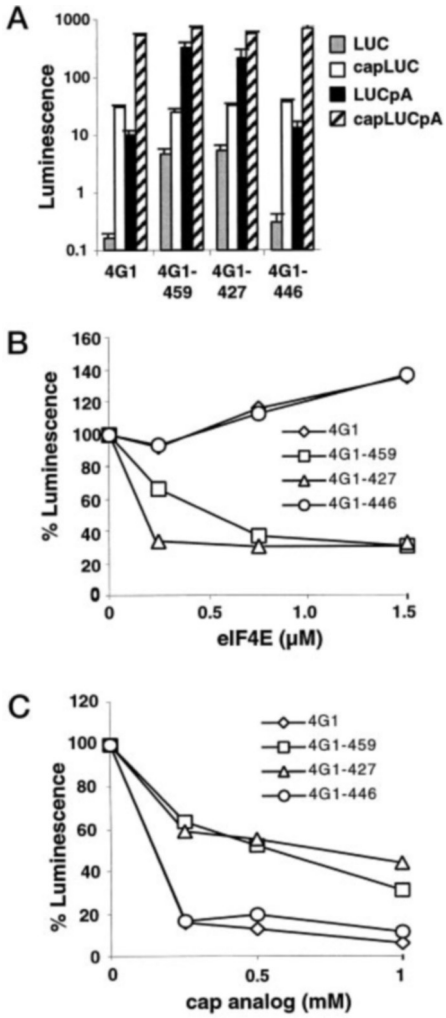

FIG. 4. **Translation extracts derived from the eIF4G1–427 and -459 mutants exhibit similar properties.** *A,* translation of uncapped mRNA is stimulated in the eIF4G1–427 extract. Non-nuclease-treated translation extracts from yeast strains YAS2421–2424 were programmed with 200 ng of capLUC, LUCpA, capLUCpA, LUC. The average luminescence value recorded from an aliquot of each translation mixture is shown. *B,* suppression of uncapped mRNA translation in the eIF4G1–427 extract by the addition of excess recombinant eIF4E. Translation extracts used in *A* were programmed with LUCpA and the indicated amount of yeast eIF4E prior to starting the reaction. The percentage of translation of the mRNA in each extract relative to that observed in the absence of eIF4E is shown. *C,* translation of capLUC mRNA in the eIF4G1–427 extract is less sensitive to the addition of excess cap analog. Translation extracts used in *A* were programmed with capLUC mRNA and the indicated amount of the cap analog m^7GpppG prior to starting the reaction. The percentage of translation of the mRNA in each of the extracts relative to that observed in the absence of the cap analog is shown.

pression to that found in the wild type extract).

The sensitivity of each extract to excess eIF4E also was examined (Fig. 4*B*). Translation of uncapped mRNA (*i.e.* LUCpA) was significantly diminished in the eIF4G1–427 extract when eIF4E was added, and the degree of translation inhibition was similar to that seen with the eIF4G1–459 extract. In contrast, the translation of LUCpA mRNA in both the wild type and eIF4G1–446 extracts was not inhibited by excess eIF4E.

The sensitivity of capLUC mRNA translation to cap analog in each extract also was measured (Fig. 4*C*). This analog nearly completely inhibited the translation of capLUC mRNA in the wild type and eIF4G1–446 extracts. In contrast, both the eIF4G1–427 and -459 extracts were less sensitive to the presence of excess cap analog. These data, in combination with the previous characterization of the eIF4G1–459 mutant (17), suggest that the eIF4G1–427 mutation reduces the interaction of eIF4G1 with eIF4E in the translation extract. They also suggest that the interaction of eIF4E with eIF4G1–446 is not disturbed to a large enough degree to exhibit changes in the translational properties of the extract.

Several methods have been developed to assay for the association of eIF4G with eIF4E in crude lysates and in mixtures containing recombinant proteins (17). Co-immunoprecipitation of eIF4E with HA epitope-tagged eIF4G from crude lysates has been shown to be sensitive to mutations that disrupt this interaction. This property is highlighted here with the eIF4G1–459 protein, which exhibits markedly decreased association with eIF4E (Fig. 5*A*). The eIF4G1–427 protein also exhibited decreased association with eIF4E relative to that seen with wild type eIF4G1. An intermediate reduction in eIF4E co-immunoprecipitation was observed with the eIF4G1–446 mutant protein. These data indicate that both the eIF4G1–427 and -446 proteins have reduced affinities for eIF4E.

The association of eIF4E and eIF4G1 was also measured using recombinant proteins (17). In one of these assays, recombinant eIF4G1 fused to the glutathione *S*-transferase protein (GST) at its N terminus was immobilized on glutathione-agarose resin and incubated with recombinant eIF4E. After washing the resin to remove unbound eIF4E, bound proteins were eluted in SDS, resolved by SDS-PAGE, and detected by Western analysis. In this assay, the GST-eIF4G1–459 protein failed to bind to eIF4E (17) (Fig. 5*B*). GST-eIF4G1–427 protein also exhibited reduced binding to eIF4E, but GST-eIF4G1–446 protein bound eIF4E at wild type levels. A similar inability to detect changes in eIF4E binding by the eIF4G2–430 protein, which has decreased affinity for eIF4E, has been reported (17). This result may reflect the low sensitivity of the assay, which uses high concentrations of each protein and may suppress the ability to detect mild alterations in binding affinities.

Far Western analysis has also been used to examine the ability of eIF4G1 to bind to eIF4E (17). In this procedure, recombinant forms of eIF4G1 were resolved by SDS-PAGE, transferred to nitrocellulose, and then probed with eIF4E. The amount of eIF4E bound to the eIF4G proteins in each lane was determined by staining the blot with antibodies to eIF4E. The GST-eIF4G1–459 protein failed to bind to eIF4E under the conditions of the experiment, whereas wild type eIF4G1 bound well (17) (Fig. 5*C*). Binding of eIF4E to eIF4G1–427 was also undetectable with this assay, in contrast to the GST-eIF4G1–446 protein, which exhibited partial eIF4E binding. These data suggest that eIF4G1–427, as well as eIF4G1–446, have decreased affinities for eIF4E.

The data presented in Figs. 3–5 are consistent with the hypothesis that the eIF4G1–427 and -446 proteins exhibit diminished binding to eIF4E. The eIF4G1–427 protein appears to be the more severely compromised because it exhibits reduced eIF4E association in each of the assays. In contrast, the eIF4G1–446 protein shows wild type activity in the translation extracts and the immobilized GST-eIF4G1 assays, a mild reduction in eIF4E affinity in both the co-immunoprecipitation and far Western assays, and a significant genetic interaction with cdc33–1p in the synthetic lethality assay. These data highlight the various sensitivities of each of the assays and underscore the importance of examining eIF4G mutations in multiple ways. Overall, the data support the conclusion that charge-to-alanine mutations at positions 427/428 and 446/447 in eIF4G1 reduce eIF4E binding.

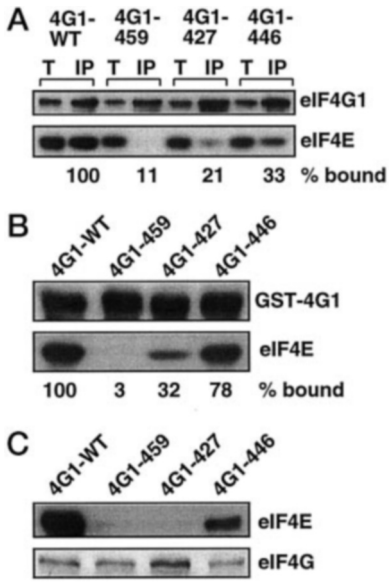

FIG. 5. **Decreased binding of eIF4E to eIF4G1–427 and -446 is observed *in vitro*.** *A,* co-immunoprecipitation of eIF4E with eIF4G1 from yeast extracts. HA epitope-tagged eIF4G1 proteins were immunoprecipitated with the 12CA5 monoclonal antibody from the extracts from strains YAS2421–2423 and YAS2137 and resolved by SDS-PAGE. The amounts of eIF4G1 and eIF4E in 0.8% of the total reaction (*T*) and in 10% of the immunoprecipitate (*IP*) were determined by Western analysis with eIF4G1- or eIF4E-specific antibodies. % bound = (eIF4E signal/eIF4G1 signal)$_{mutant}$/(eIF4E signal/eIF4G1 signal)$_{wild\ type}$. Signal intensities were determined using a Molecular Dynamics chemifluorescence scanner. *B,* binding of recombinant eIF4E to immobilized GST-eIF4G1 fusion proteins. The indicated GST-eIF4G1 fusion proteins were immobilized on glutathione-agarose beads and incubated with 25 μg/ml of recombinant eIF4E. Following extensive washing of the resin, bound proteins were eluted with SDS, resolved by SDS-PAGE, and visualized by Western analysis using anti-eIF4G1 and anti-eIF4E antibodies. The percentage bound was determined as described in *A*. *C,* far-Western analysis of immobilized GST-eIF4G1 binding to soluble eIF4E. The indicated GST-eIF4G1 fusion proteins were resolved by SDS-PAGE, transferred to nitrocellulose, and probed with 1 μg/ml of recombinant eIF4E. Following extensive washing of the filter, the eIF4E bound to eIF4G was detected by Western analysis with anti-eIF4E antibodies. The amount of GST-eIF4G1 in each lane of an identical SDS-PAGE gel was determined by Coomassie Brilliant Blue staining.

DISCUSSION

We report here that a 98-residue fragment of eIF4G1 is protected from protease degradation in the presence but not the absence of eIF4E. This region, which spans amino acids 393–490 and contains the eIF4E binding peptide, was determined by NMR spectroscopy to be unstructured in the absence of eIF4E and largely folded in the presence of eIF4E. Charge-to-alanine mutations at positions 427/428 and 446/447 in the full-length eIF4G1 protein diminished the ability of eIF4G1 to interact with eIF4E both *in vivo* and *in vitro*. In total, these data support the hypothesis that residues in eIF4G1 surrounding the eIF4E binding peptide help mediate high affinity eIF4E binding.

Previous studies on the physical interaction between eIF4E and eIF4G or the 4E-BPs have used short peptides (17 or 20 amino acids) to identify important residues in this interaction (29).[2] Although these studies have generated important data regarding the interaction of eIF4E with eIF4G, there is uncertainty as to whether these are the only interactions that occur with the full-length eIF4G. The work presented here begins to address this issue. The discovery of a protease-resistant fragment of eIF4G1 in the presence of eIF4E could suggest that many contacts are made between these two proteins. However, two other observations suggest this cannot be the full explanation. First, most of the highly conserved surface of eIF4E not bound to the cap structure is masked by a 17-amino acid fragment containing the eIF4E binding peptide.[2] Second, our NMR experiments revealed an unfolded to folded transition of eIF4G1$_{393–490}$ upon binding to eIF4E. Therefore, we believe that the protease resistant fragment of eIF4G1 arises from a combination of new contacts with eIF4E and sequestration of protease sites within the folded domain.

The discovery of two mutations from a set of 24 charge-to-alanine mutants throughout most of the eIF4G1 protein that lie within the stabilized 98-amino acid fragment emphasize the importance of the domain in the binding of eIF4G1 to eIF4E. However, they provide no insight into the relative contributions of new contacts *versus* folding in creating a protease resistant fragment. This is because the mutations could remove residues involved in either direct contact with eIF4E or proper folding of the eIF4G1 domain. This latter possibility also suggests that there could be many other mutations within eIF4G1 that reduce binding to eIF4E by preventing its folding. The determination of the three dimensional structure of the 98-residue domain of eIF4G1 bound eIF4E will be necessary before further interpretations of our data can be made.

Several recent reports have addressed the similarities and differences between eIF4G and 4E-BP binding to eIF4E. Based on the x-ray crystallographic structure of a 17-amino acid peptide from 4E-BP1 bound to eIF4E[2] and the conservation of residues between 4E-BP1 and eIF4G that contact eIF4E (16), it has been suggested that these two proteins associate with eIF4E in nearly identical ways. In contrast, it has been noted that mutations within eIF4E that diminish eIF4G1$_{348–513}$ binding have a much less severe effect on Caf20p binding (19).

The data presented in this report may provide some explanation for these discrepancies between studies on model peptides and larger fragments of eIF4E-associated proteins. Binding to eIF4E has different consequences for 4E-BP1, which remains largely unstructured (29), and eIF4G1$_{393–490}$, which folds upon binding. The folding of eIF4G1$_{393–490}$ could enhance its affinity for eIF4E both directly, by introducing new contacts between the two proteins, or indirectly, by releasing the eIF4E binding peptide from an inaccessible state. New contacts, even if they were nonspecific, could substantially increase binding, especially if they were geometrically favored by the folded structure adopted by eIF4G1$_{393–490}$. In contrast, because 4E-BP1 remains largely unstructured outside of the conserved binding site upon eIF4E binding, no such additional contacts would contribute to binding.

The findings that much of the eIF4G1$_{393–490}$ fragment is folded upon binding to eIF4E and that mutations within this fragment diminish eIF4E binding suggest possible ways that eIF4G binding to eIF4E could be regulated to control translation initiation. One possible means of regulation is to decrease the free energy difference between the unfolded and folded states of eIF4G by modifications such as phosphorylation or by the binding of another protein to folded eIF4G1. This would have the effect of increasing the affinity of eIF4G for eIF4E by stabilizing the folded conformation of the eIF4G1$_{393–490}$ domain. One likely candidate for such a protein is the poly(A) tail-binding protein Pab1p, which binds to a region of eIF4G just N-terminal to the eIF4E binding region and, in conjunction with eIF4E, activates 40 S ribosomal subunit binding to the mRNA (10, 28). If Pab1p stabilizes the folded form of eIF4G, this could explain the observed synergistic activation of translation observed when both eIF4E and Pab1p are bound to eIF4G. Conversely, it is also possible that eIF4G binding to eIF4E is negatively regulated by proteins or covalent modifications that prevent residues within eIF4G from folding. For

instance, phosphorylation of residues within this region could favor the unfolded state of the $eIF4G1_{393-490}$ domain. Future work will be needed to more directly address each of these possible regulatory mechanisms.

The induction of a unique structure within eIF4G1 upon binding to eIF4E could lead to the exposure of new surfaces on eIF4G1 that have distinct functions in translation. Such allosteric control of eIF4G would mean that eIF4G in the absence of eIF4E has different biochemical properties than in its presence. Several recent observations lend support to this hypothesis. First, the cleavage of human eIF4G1 by picornavirus proteases is activated when it is bound to eIF4E (31, 32). Second, translation extracts containing eIF4G proteins with low affinity for eIF4E exhibit high levels of uncapped mRNA translation, and this effect can be reversed by excess eIF4E (see above and Ref. 17). In the presence of eIF4E, the structural rearrangement of eIF4G may lead to binding of some other component of the initiation complex, such as an mRNA-bound protein or a ribosome-associated protein, and this could both enhance the efficiency of recruitment or retention of the initiation complex as well as its protease-sensitivity. Alternatively, the newly formed surface may repress an activity of eIF4G, such as RNA-binding and cap-independent translation. Future studies will need to determine whether mutations like eIF4G1–446, which only mildly affect binding to eIF4E but show strong genetic interactions with eIF4E mutations *in vivo*, alter these proposed functions of the eIF4E-dependent surface on eIF4G.

It is important to note that many of these conclusions are based upon the assumption that amino acids 393–490 in the full-length eIF4G1 protein are also unfolded in the absence of eIF4E. Although the phenotypes associated with the eIF4G1–427 and -446 mutations within the full-length protein are consistent with our conclusions from studies using eIF4G fragments, it will be necessary in future studies to determine the structure of this region within the full-length protein in the absence and presence of eIF4E.

In summary, we have presented biophysical, biochemical, and genetic evidence that a 98-amino acid domain of eIF4G1 contains residues necessary for high affinity eIF4E binding and becomes extensively structured in the presence of eIF4E. This domain may contribute to the effects of eIF4G1 on eIF4E function and may provide a new binding surface for other effectors of the translation initiation apparatus. Future work examining the structure of eIF4G and eIF4E in greater detail, as well as the functional consequences of their interactions upon the translation initiation process, should yield more insight into each of these issues.

Acknowledgments—We thank David King for the mass spectrometry, Sharleen Zhou for microsequencing, and Jennifer Blanchette for sharing of reagents. P. E. C. Hershey and A. B. Sachs thank members of their laboratory for critical reading of the manuscript.

REFERENCES

1. Mathews, M. B., Sonenberg, N., and Hershey, J. W. B. (1996) in *Translational Control* (Hershey, J. W., Mathews, M. B., and Sonenberg, N., eds) Vol. 30, pp. 1–29, Cold Spring Harbor Laboratory, Cold Spring Harbor, NY
2. Shatkin, A. J. (1976) *Cell* **9,** 645–653
3. Sonenberg, N., and Gingras, A.-C. (1998) *Curr. Opin. Cell Biol.* **10,** 268–275
4. Merrick, W. C., and Hershey, J. W. B. (1996) in *Translational Control* (Hershey, J. W. B., Mathews, M., and Sonenberg, N., eds) Vol. 30, pp. 31–69, Cold Spring Harbor Laboratory, Cold Spring Harbor, NY
5. Morley, S. J., Curtis, P. S., and Pain, V. M. (1997) *RNA* **3,** 1085–1104
6. Feigenblum, D., and Schneider, R. J. (1996) *Mol. Cell. Biol.* **16,** 5450–5457
7. Pyronnet, S., Imataka, H., Gingras, A.-C., Fukunaga, R., Hunter, T., and Sonenberg, N. (1999) *EMBO J.* **18,** 270–279
8. Brenner, C., Nakayama, N., Goebl, M., Tanaka, K., Toh-e, A., and Matsumoto, K. (1988) *Mol. Cell. Biol.* **8,** 3556–3559
9. Goyer, C., Altmann, M., Lee, H. S., Blanc, A., Deshmukh, M., Woolford, J. L., Trachsel, H., and Sonenberg, N. (1993) *Mol. Cell. Biol.* **13,** 4860–4874
10. Tarun, S. Z., and Sachs, A. B. (1996) *EMBO* **15,** 7168–7177
11. Altmann, M., Sonenberg, N., and Trachsel, H. (1989) *Mol. Cell. Biol.* **9,** 4467–4472
12. Goyer, C., Altmann, M., Trachsel, H., and Sonenberg, N. (1989) *J. Biol. Chem.* **264,** 7603–7610
13. Altmann, M., Schmitz, N., Berset, C., and Trachsel, H. (1997) *EMBO J.* **16,** 1114–1121
14. Cruz, J., Iost, I., Kressler, D., and Linder, P. (1997) *Proc. Natl. Acad. Sci. U. S. A.* **94,** 5201–5206
15. Zanchin, N. I. T., and McCarthy, J. E. G. (*1995*) *J. Biol. Chem.* **270,** 26505–26510
16. Mader, S., Lee, H., Pause, A., and Sonenberg, N. (1995) *Mol. Cell. Biol.* **15,** 4990–4997
17. Tarun, S. Z., and Sachs, A. B. (1997) *Mol. Cell. Biol.* **17,** 6876–6886
18. Lang, V., Zanchin, N., Lunsdorf, H., Tuite, M., and McCarthy, J. E. G. (1994) *J. Biol. Chem.* **269,** 6117–6123
19. Ptushkina, M., von der Haar, T., Vasilescu, S., Frank, R., Birkenhager, R., and McCarthy, J. E. G. (1998) *EMBO J.* **17,** 4798–4808
20. Haghighat, A., and Sonenberg, N. (1997) *J. Biol. Chem.* **272,** 21677–21680
21. Lamphear, B. J., Kirchweger, R., Skern, T., and Rhoads, R. E. (1995) *J. Biol. Chem.* **270,** 21975–21983
22. Imataka, H., and Sonenberg, N. (1997) *Mol. Cell. Biol.* **17,** 6940–6947
23. Vasilescu, S., Ptushkina, M., Linz, B., Muller, P. P., and McCarthy, J. E. G. (1996) *J. Biol. Chem.* **271,** 7030–7037
24. Edery, I., Altmann, M., and Sonenberg, N. (1988) *Gene* **74,** 517–525
25. Barettino, D., Feigenbutz, M., Valcarcel, R., and Stunnenberg, H. G. (1993) *Nuc. Acids Res.* **22,** 541–542
26. Guthrie, C., and Fink, G. (1991) *Guide to Yeast Genetics and Molecular Biology: Methods in Enzymology* (Abelson, J., and Simon, M. I., eds) Vol. 194, pp. 14–15, Academic Press, San Diego, CA
27. Boeke, J. D., Trueheart, J., Natsoulis, G., and Fink, G. (1987) *5-Fluoroorotic Acid as a Selective Agent in Yeast Molecular Genetics: Methods in Enzymology* (Abelson, J., and Simon, M. I., eds) Vol. 154, pp. 164–175, Academic Press, San Diego, CA
28. Tarun, S., and Sachs, A. B. (1995) *Genes Dev.* **9,** 2997–3007
29. Fletcher, C. M., McGuire, A. M., Gingras, A.-C., Li, H., Matsuo, H., Sonenberg, N., and Wagner, G. (1998) *Biochemistry* **37,** 9–15
30. Tarun, S. Z., Wells, S. E., Deardorff, J. A., and Sachs, A. B. (1997) *Proc. Natl. Acad. Sci. U. S. A.* **94,** 9046–9051
31. Haghighat, A., Svitkin, Y., Novoa, I., Kuechler, E., Skern, T., and Sonenberg, N. (1996) *J. Virol.* **70,** 8444–8450
32. Ohlmann, T., Pain, V. M., Wood, W., Rau, M., and Morley, S. J. (1997) *EMBO J.* **16,** 844–855